ELSEVIER

Contents lists available at SciVerse ScienceDirect

Journal of Alloys and Compounds

journal homepage: www.elsevier.com/locate/jalcom



A facile template-free route to synthesize porous ZnO nanosheets with high surface area



Xiulan Hu^{a,*}, Xiaodong Shen^a, Rong Huang^b, Yoshitake Masuda^c, Tatsuki Ohji^c, Kazumi Kato^c

- ^a College of Materials Science and Engineering, Nanjing University of Technology, Xin-mo-fan Road No. 5, Nanjing 210009, China
- ^b Key Laboratory of Polar Materials and Devices, Ministry of Education, East China Normal University, Shanghai 200062, China
- ^c National Institute of Advanced Industrial Science and Technology (AIST), 2266-98 Anagahora, Shimoshidami, Moriyama-ku, Nagoya 463-8560, Japan

ARTICLE INFO

Article history:
Received 11 April 2013
Received in revised form 11 June 2013
Accepted 14 June 2013
Available online 25 June 2013

Keywords: ZnO Porous materials Nanosheets Chemical deposition

ABSTRACT

Microporous and mesoporous ZnO nanosheets were successfully synthesized by a low-temperature chemical bath deposition and subsequently thermal decomposition at 250 °C without any templates. Nanosheet-shaped zinc hydroxide nitrate $(Zn_3(OH)_4(NO_3)_2)$ was formed as the precursors at 90 °C for 6 days by chemical bath deposition in a close system. Microporous and mesoporous ZnO nanosheets were obtained from the removing of OH and NO_3 groups from zinc hydroxide nitrate $(Zn_3(OH)_4(NO_3)_2)$ nanosheet-shaped precursors. The pore sizes were distributed in the region of $\sim 1.3-25$ nm with a center at ~ 2.4 nm. Such porous and nanosheets structure gave a highest specific surface area of 283.8 m²/g.

© 2013 Elsevier B.V. All rights reserved.

1. Introduction

Mesoporous semiconductors offer great interest for their vast ability to adsorb and interact with atoms, ions and molecules on their wide interior surface and in the nanometer pore size. Porous semiconductor photocatalysts are attractive in the applications such as bioengineering and photocatalysis, through minimizing the distance between the site of photon absorption and electron/hole redox reactions to improve efficiency [1].

Semiconductor zinc oxide (ZnO) is used in a wide range of functional devices, nanostructure varistors, UV absorbers, gas sensors, biosensor, photocatalysts, dye-sensitized solar cells, piezoelectric devices, light-emitting diodes, field emission flat panel displays and photodiodes and industrial additives due to its wide band gap (3.37 eV) with large exciton binding energy (60 meV) [2-6]. Porous ZnO nanostructures for optimized performance of dye-sensitized photovoltaic cells, hydrogen storage, catalysis, and secondary batteries have recently attracted significant research interest. Clearly, the formations of porous materials with tailored properties are still challenging, and therefore, there is significant interest in the development of methods using a template-technique that can yield materials with various pore sizes and morphologies. Porous ZnO has been synthesized by several methods, such as dip-coating [7] or electrochemical deposition [8] with a polystyrene (PS) template, or a copolymer gel template (hydroxyl ethyl methacrylate (HEMA) and ethylene glycol dimethacrylate (EGDMA)) (SBET - $\approx 65-115 \text{ m}^2/\text{g}$) [9], or a self-assembly pathway in aqueous solution using surface-modified colloidal ZnO nanocrystallites as the building blocks and P-123 copolymers as the template (S_{BET} - $\approx 45 \text{ m}^2/\text{g}$) [1], in situ precipitation using poly(acrylic acid) (PPA) membranes (the size of crystals and the pores are about 5-10 nm) [10], exotemplating with mesoporous carbon (S_{BET} - $\approx 200 \text{ m}^2/\text{g})$ [11], or in situ hydrolysis of Zn(CH₃COO)₂ • 2H₂O in LiOH-ethanol solution combined with templating anneal of mesoporous precursors (Octadcylamine, Pluronic F-127, Pluronic P-123) at 600 °C for 5 h ($S_{BET} \approx 69-100 \text{ m}^2/\text{g}$) [12]. It is obviously that the template-technique faced a removal problem of template by high temperature calcination or poisonous organic solvent for getting high purity ZnO products. And porous ZnO nanowires were reported to obtained by thermal oxidation of ZnSe precursor at 700 °C for 1 h [13]. Recently, chemical bath deposition (CBD) technique has attracted considerable attention due to its many advantages such as simple procedure, low energy demand and cost, also environmental friendly. Porous ZnO is prepared through 300 °Cthermal decomposition of synthesized zinc carbonate hydroxide by chemical bath deposition (CBD) process without any template (nanoparticles size are about 10-20 nm) [14]. Recently novel hierarchical porous ZnO microspheres assembled by porous nanosheets $(S_{BET} \approx 39.6 \text{ m}^2/\text{g})$ are synthesized from zinc hydroxide carbonate [Zn₄(CO₃)(OH)₆] precursor fabricated in hydrothermal autoclave. [15] However, it is difficult to obtain porous ZnO with high surface area. In this study, we describe the high yield preparation of microporous and mesoporous ZnO nanosheets with high

^{*} Corresponding author. Tel./fax: +86 25 8368 7260. E-mail address: whoxiulan@163.com (X. Hu).

specific surface ($S_{BET} \approx 283.8 \text{ m}^2/\text{g}$) using a simple chemical deposition without any template assistant. The formation mechanism and crystalline structure and morphology were characterized.

2. Experimental section

A 200-ml aqueous solution of zinc nitrate hexahydrate $(Zn(NO_3)_2\cdot 6H_2O, 99\%, Wako, Japan)$ and hexamethylenetetramine $(C_6H_{12}N_4, 99\%, Wako, Japan)$ was prepared as a precious solution. The initial concentration of free Zn^{2+} was fixed to 0.2 mol/L. The molar ratio was fixed to 1:1, respectively. Subsequently, the precious solution was transferred into a 300 ml-autoclave at room temperature. The autoclave was kept in an oven at 90 °C for 6 days. After the desired deposition time, the precipitations were harvested and washed repeatedly with deionized water, and then air-dried at room temperature. Finally, a transformation into ZnO was conducted by heating the precipitations at 250 °C in air atmosphere for 1 h by heating rate of 10 °C per minute for characterization.

The crystalline phase of products were identified using X-ray diffraction (XRD; RINT-2100V, Rigaku) with Cu Kα radiation (40 kV, 30 mA) and scan rate of 2 °/min. The morphology and microstructure were observed using a field emission scanning electron microscope (FE-SEM: ISM-6335FM, IEOL Ltd.) with accelerating voltage of $5\,kV$ and emission current of $12\,\mu A$ and a high-resolution transmission electron microscope (HR-TEM; JEM-3000 F, JEOL, Topcon Ltd.). Nitrogen (N2) adsorptiondesorption isotherms were obtained using autosorb-1 (Quantachrome Instruments) after samples was outgassed at 110 °C under 10⁻² mmHg for 6 h. Specific surface area was calculated by the Brunauer-Emmet-Teller (BET) method using desorption isotherms. The photocatalytic activity was evaluated by examining photocatalytic degradation of ethylene blue (MB) as a representative dye pollutant. 0.4 g/l ZnO powder were dispersed in an aqueous solution containing 20 mg/l MB. The solutions were irradiated with visible light through a glass filter using an ultra-high pressure mercury lamp (wavelength: 410-600 nm, multilight UIV-270, Ushio, Japan). The concentration change of MB by photocatalytic degradation was evaluated by monitoring 650 nm absorbance using an UV-vis light spectrometer (U-4100, Hitachi, Japan).

3. Results and discussion

Fig. 1a shows the XRD pattern of as-deposited products in an aqueous solution at 90 °C for 6 days. Zinc hydroxide nitrate ($Zn_3(-OH)_4(NO_3)_2$, JCPDS card No. 52-0627) were detected as main phases. $Zn_3(OH)_4(NO_3)_2$ belongs to the monoclinic (P21/c(14)) with $2\theta \approx 12.8$ at (100) peak, the diffraction peaks were marked by the Miller index as shown in Fig. 1a. Fig. 1b shows the XRD pattern of product obtained after heating at 250 °C for 1 h, all of diffraction peaks are in good agreement with the JCPDS card (No. 36-1451) for a typical wurtzite-type ZnO crystal (hexagonal, $P6_3mc$) and no impurity phases were detected. The full width at half maximum of X-ray diffraction peaks become slightly broadened, indicating the formation of ZnO nanoparticles by thermal decomposition of $Zn_3(OH)_4(NO_3)_2$ phase.

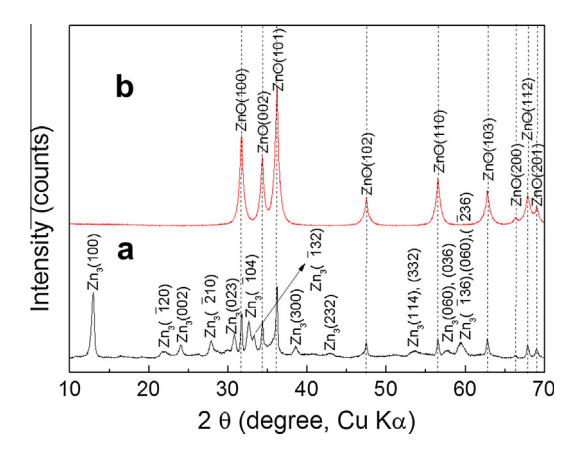


Fig. 1. XRD patterns of products. (a) As-deposited products; (b) 250 °C-heated products (references for zinc nitrate hydroxide and zinc oxide according to Jade PDF code are 52-0627 ($Zn_3(OH)_4(NO_3)_2$, abbreviated as Zn_3), and 36-1452 (ZnO), respectively).

(References for zinc nitrate hydroxide and zinc oxide according to Jade PDF code are 52-0627 ($Zn_3(OH)_4(NO_3)_2$, abbreviated as Zn_3), and 36-1452 (ZnO), respectively).

Fig. 2 shows the FE-SEM images of as-deposited $Zn_3(OH)_4(NO_3)_2$ phase and ZnO obtained by 250 °C heat-treatment. As-deposited $Zn_3(OH)_4(NO_3)_2$ phase are shaped as nanosheets. After heating at 250 °C for 1 h, NO_3 and OH group in $Zn_3(OH)_4(NO_3)_2$ phase were facile removed through the thermal decomposition, nanosheet-shaped and porous ZnO were obtained.

As obtained precursor Zn₃(OH)₄(NO₃)₂ nanosheets gave a BET surface areas of about 50 m²/g. The BET surface areas resulting from the nanosheet morphology was lower. While ZnO nanosheets deriving from thermal decomposition of precursor Zn₃(OH)₄(NO₃)₂ exhibited N₂ adsorption-desorption isotherms of Type IV as shown in Fig. 3a. The desorption isotherm differed from adsorption isotherm in the relative pressure (P/P_0) range of 0.70–0.97. The hysteretic behavior may be explained by both connectivity and the broadening of the pore size distribution in porous materials. The hysteresis area increases with the standard deviation of the pore size distribution. Thus smaller hysteresis area results clarified that obtained ZnO products have a small pore size distribution. Specific surface area was calculated by the Brunauer-Emmett-Teller (BET) method using adsorption isotherms. The BET surface area (S_{BET}) of the particles was estimated to be 283.8 m²/g by the BET surface area plot in the relative pressure (P/P_0) range of 0.10-0.30 as shown in Fig. 3b. The value of S_{BET} was significantly higher than that of commercial ZnO nanoparticles with the size of 30-40 nm (NanoTek®ZnO, 30 m²/g, Japan) and other porous ZnO samples reported by Polarz et al. [11] ($S_{BET} \approx 200 \text{ m}^2/\text{g}$) and Yan et al. [12] $(S_{BET} \approx 70-100 \text{ m}^2/\text{g})$ prepared by the templating techniques. Because capillary condensation occurs at relatively higher pressure, desorption branch is used to evaluate the pore size of ZnO by the BJH method. The analysis (inset in Fig. 3b) provides one peak centered at \sim 2.4 nm in the pore size distribution in the region of \sim 1.3– 25 nm. Fig. 4a shows a typical transmittance microscope of as-prepared ZnO, it well confirmed ZnO are nanosheets morphology. A high-resolution transmission electron microscope (HR-TEM) as shown in Fig. 4b indentified ZnO nanosheets were porous structure and good crystalline. Thus the BET and HR-TEM results indentified porous ZnO nanosheets have micropores and mesopores. These micropores and mesoporous derive from the removal of OH and NO₃ group from Zn₃(OH)₄(NO₃)₂ nanosheets by thermal decomposition at 250 °C. Therefore such microporous and mesoporous, and nanosheet structure gave a high BET surface area. As it was well known, nanostructures with a higher surface area should work as better photocatalysts, sensor and solar cells. Thus as-prepared porous ZnO nanosheets will find a potential wide variety application in a nano-scaled electronic and optoelectronic device, and photocatalyst.

Fig. 5 shows UV–vis spectra from the 20 mg/L MB solution with the porous ZnO nanosheets (400 mg/L) at different time intervals (a), and MB degradation curves of the (C_t/C_0) versus irradiation time for photodegradation with the ZnO samples (b). The absorption peak at 650 nm corresponding to MB molecule quickly decreases with the exposure time within 40 min. After 30 min UV irradiation, almost 90% of MB molecules are decomposed in the presence of the ZnO sample. This observation is quite different from that without the ZnO sample and as-reported ZnO products. Thus these results show as-synthesized ZnO have higher photocatalytic activity, due to porosity and nanosheets provide more active sits for MB absorption and degradation.

According to our initial stage research work, the formation of $Zn_3(OH)_4(NO_3)_2$ nanosheets were discussed as the follow: in the zinc nitrate – HMT system, HMT, which is extensively used in the fabrication of ZnO nanostructures [16–19], provided the ammonia molecules (NH_3) and hydroxide ions (OH^-) to the

Download English Version:

https://daneshyari.com/en/article/1613219

Download Persian Version:

https://daneshyari.com/article/1613219

Daneshyari.com